depend on the specific molecular-scale solvent-substrate interactions.

References and Notes

1. A. Fujishima, K. Honda, *Nature* **238**, 37 (1972).
2. M. Grätzel, *Nature* **414**, 338 (2001).
3. M. A. Fox, M. T. Dulay, *Chem. Rev.* **93**, 341 (1993).
4. R. Wang *et al.*, *Nature* **388**, 431 (1997).
5. P. V. Kamat, *Chem. Rev.* **93**, 267 (1993).
6. K. Onda *et al.*, *Science* **308**, 1154 (2005).
7. J. Zhao, B. Li, K. D. Jordan, J. Yang, H. Petek, in preparation.
8. H. Tributsch, L. Pohlmann, *Science* **279**, 1891 (1998).
9. R. I. Cukier, D. G. Nocera, *Annu. Rev. Phys. Chem.* **49**, 337 (1998).
10. S. Hammes-Schiffer, *Acc. Chem. Res.* **34**, 273 (2001).
11. M. S. Pshenichnikov, A. Baltuska, D. A. Wiersma, *Chem. Phys. Lett.* **389**, 171 (2004).
12. C. Tanner, C. Manca, S. Leutwyler, *Science* **302**, 1736 (2003).
13. J. Lin, I. A. Balabin, D. N. Beratan, *Science* **310**, 1311 (2005).
14. X. Shi, F. H. Long, H. Lu, K. B. Eisenthal, *J. Phys. Chem.* **99**, 6917 (1995).
15. H. Shirota, K. Yoshihara, N. A. Smith, S. Lin, S. R. Meech, *Chem. Phys. Lett.* **281**, 27 (1997).
16. M. J. Tauber, C. M. Stuart, R. A. Mathies, *J. Am. Chem. Soc.* **126**, 3414 (2004).
17. P. Minary, L. Turi, P. J. Rossky, *J. Chem. Phys.* **110**, 10953 (1999).
18. L. Turi, *J. Chem. Phys.* **110**, 10364 (1999).
19. S. H. Liu *et al.*, *J. Phys. Chem. B* **106**, 12908 (2002).
20. M. A. Henderson, S. O. Tapia, M. E. Castro, *Fara. Disc.* **114**, 313 (1999).
21. S. P. Bates, M. J. Gillan, G. Kresse, *J. Phys. Chem. B* **102**, 2017 (1998).
22. T. Kawai, T. Sakata, *J. Chem. Soc. Chem. Commun.* 694 (1980).
23. K. Onda, B. Li, H. Petek, *Phys. Rev. B* **70**, 045415 (2004).
24. K. Onda, B. Li, J. Zhao, H. Petek, *Surf. Sci.* **593**, 32 (2005).
25. H. Petek, S. Ogawa, *Prog. Surf. Sci.* **56**, 239 (1997).
26. The calculations were carried out by using the generalized gradient approximation (GGA) based on DFT. At the GGA level, we choose the Perdew-Burke-Ernzerhof functional (*27*, *28*), together with the double numerical atomic orbitals augmented by polarization functions (DNP), as the basis functions and the density functional semi-core pseudopotential (DSPP). Self-consistent field procedures were done with a convergence criterion of 10^{-6} atomic units (au) on the energy and electron density. Geometry optimizations were performed with a convergence criterion of 10^{-3} au on the gradient, 10^{-3} au on the displacement, and 10^{-5} au on the energy. All the calculations were carried out using the molecular simulation package DMOL3 [DMOL3 is a DFT-based package with atomic basis distributed by Accelrys (*29*)].
27. J. P. Perdew, K. Burke, M. Ernzerhof, *Phys. Rev. Lett.* **78**, 1396 (1997).
28. J. P. Perdew, K. Burke, M. Ernzerhof, *Phys. Rev. Lett.* **77**, 3865 (1996).
29. B. Delley, *J. Chem. Phys.* **92**, 508 (1990).
30. B. Li, K. Onda, H. Petek, data not shown.
31. M. J. Weida, S. Ogawa, H. Nagano, H. Petek, *J. Opt. Soc. Am. B* **17**, 1443 (2000).
32. E. Hendry, F. Wang, J. Shan, T. F. Heinz, M. Bonn, *Phys. Rev. B* **69**, 081101 (2004).
33. H. Decornez, S. Hammes-Schiffer, *J. Phys. Chem. A* **104**, 9370 (2000).
34. W. Stier, O. V. Prezhdo, *J. Phys. Chem. B* **106**, 8047 (2002).
35. L. G. C. Rego, V. S. Batista, *J. Am. Chem. Soc.* **125**, 7989 (2003).
36. R. Monnier, J. P. Perdew, D. C. Langreth, J. W. Wilkins, *Phys. Rev. B* **18**, 656 (1978).
37. R. O. Jones, O. Gunnarsson, *Rev. Mod. Phys.* **61**, 689 (1989).
38. The excited state prepared in the experiment corresponds to an electron in the CH_3OH overlayer and a hole remaining at the TiO_2 surface. By adding an electron to the CH_3OH orbital to simulate the excited state, we make an assumption that the hole is screened and the excitonic effects can be ignored. Calculations where the ground state is optimized with an extra electron (the true ground state of our excited state) gave the essentially identical structure to those in Fig. 2, A and B. The success of the excited state optimization procedure relies on the molecular overlayer state being sufficiently decoupled from the surface to not decay into the conduction band of TiO_2.
39. Q. B. Lu, T. E. Madey, *Phys. Rev. Lett.* **82**, 4122 (1999).

40. This work was supported by the Department of Defense Multidisciplinary University Research Initiative program under Grant DAAD19-01-1-0619, by the New Energy Development Organization of Japan "Molecular Wire" project, by the National Science Foundation of China (grants 20533030 and 50121202), and by NSF grant CHE-0518253. The apparatus for TR-2PP has been developed with support from NSF grant DMR-0116034. We thank J. T. Yates Jr. for the donation of the CH_3OD sample.

3 November 2005; accepted 31 January 2006
10.1126/science.1122190

Observation of Feshbach Resonances in the $F + H_2 \rightarrow HF + H$ Reaction

Minghui Qiu,[1,3]* Zefeng Ren,[1]* Li Che,[1] Dongxu Dai,[1] Steve A. Harich,[1] Xiuyan Wang,[1] Xueming Yang,[1]† Chuanxiu Xu,[4] Daiqian Xie,[4]† Magnus Gustafsson,[5,6] Rex T. Skodje,[5,6] Zhigang Sun,[1,2,7] Dong H. Zhang[1,2,7]†

Reaction resonances, or transiently stabilized transition-state structures, have proven highly challenging to capture experimentally. Here, we used the highly sensitive H atom Rydberg tagging time-of-flight method to conduct a crossed molecular beam scattering study of the $F + H_2 \rightarrow HF + H$ reaction with full quantum-state resolution. Pronounced forward-scattered HF products in the $v' = 2$ vibrational state were clearly observed at a collision energy of 0.52 kcal/mol; this was attributed to both the ground and the first excited Feshbach resonances trapped in the peculiar HF($v' = 3$)-H′ vibrationally adiabatic potential, with substantial enhancement by constructive interference between the two resonances.

Dynamical resonance in chemical reactions (*1*) has attracted great attention from both experimentalists and theoreticians (*2*–*5*) over the past 30 years. In general, the transition state is an energy maximum along the reaction coordinate, and so it does not persist as a discrete structure. However, in special cases, a reaction complex in the transition-state region can be transiently trapped in vibrationally adiabatic wells along the reaction coordinate. A transiently trapped state along the reaction coordinate in the transition-state region is normally called a dynamical resonance or a Feshbach resonance. Dynamical resonance (or reaction resonance) thus constitutes an extremely sensitive probe of the potential energy surface (PES) of a chemical reaction.

The most well-studied example for dynamical resonance is the $F + H_2 \rightarrow HF + H$ reaction, which is also known to be the main pumping step for the HF chemical laser. Theoretical predictions of a reaction resonance in the $F + H_2$ reaction were first made in the 1970s (*6*–*9*). In a landmark crossed-beams experiment on the $F + H_2$ reaction in the collision energy range of 0.7 to 3.4 kcal/mol by Lee and coworkers (*10*, *11*), a forward-scattering peak for the HF($v' = 3$) product was clearly observed and was attributed to a reaction resonance. Later theoretical studies using both the quasi-classical trajectory method (*12*) and the quantum mechanical scattering method (*13*) on the Stark-Werner PES (SW-PES) (*14*), however, did not confirm this conjecture. In a recent study of the $F + HD \rightarrow HF + D$ reaction, a step in the excitation function around 0.5 kcal/mol was unambiguously observed (*15*). Concurrent theoretical analysis based on the SW-PES showed that this step is due to a H-F-D(003) resonance. Neumark and co-workers also probed the transition state of the $F + H_2$ reaction by negative ion photodetachment spectroscopy (*16*). Full quantum mechanical calculations based on the SW-PES led to nearly quantitative agreement with the FH_2^- photoelectron spectrum (*16*). The nature of the resonances observed in the FH_2^- photoelectron spectrum was analyzed by Russell and Manolopoulos (*17*).

Despite more recent experimental studies on this system (*18*, *19*), a definitive detection of reaction resonances in the $F + H_2$ reaction in a scattering experiment still remains elusive. Moreover, serious questions have been raised about the SW-PES that predicts the resonances, such as

[1]State Key Laboratory of Molecular Reaction Dynamics, [2]Center for Theoretical and Computational Chemistry, Dalian Institute of Chemical Physics, Chinese Academy of Sciences, Dalian, Liaoning 116023, P. R. China. [3]Department of Physics, Dalian Jiaotong University, Dalian, P. R. China. [4]Institute of Theoretical and Computational Chemistry, Department of Chemistry, Nanjing University, Nanjing, Jiangsu 210093, P. R. China. [5]Institute of Atomic and Molecular Sciences, Academia Sinica, P.O. Box 23-166, Taipei, Taiwan. [6]Department of Chemistry and Biochemistry, University of Colorado, Boulder, CO 80309, USA. [7]Department of Computational Science, National University of Singapore, Singapore 119260.

*These authors contributed equally to this work.
†To whom correspondence should be addressed. E-mail: xmyang@dicp.ac.cn, dqxie@nju.edu.cn, zhangdh@dicp.ac.cn

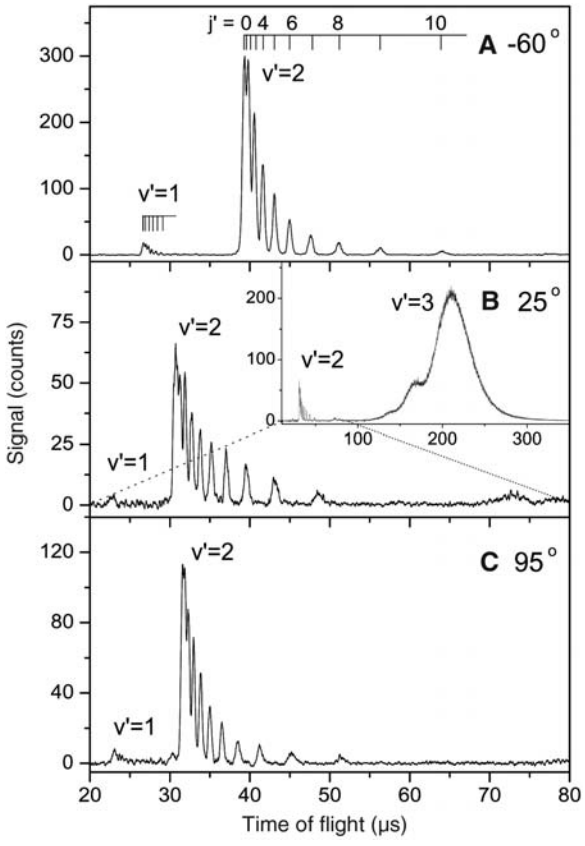

Fig. 1. TOF spectra of the H atom product from the $F(^2P_{3/2}) + H_2(j = 0)$ reaction at the collision energy of 0.52 kcal/mol. TOF spectra at three laboratory angles are shown: (**A**) $\Theta_L = -60°$, (**B**) $\Theta_L = 25°$, and (**C**) $\Theta_L = 95°$, which correspond roughly to the forward-, sideways-, and backward-scattering directions for the HF($v' = 2$) product in the center-of-mass frame, respectively. Only HF($v' = 1, 2, 3$) products are observed here. The inset in (B) also shows the formation of HF($v' = 3$), which is much more abundant than HF($v' = 2$) at this scattering angle.

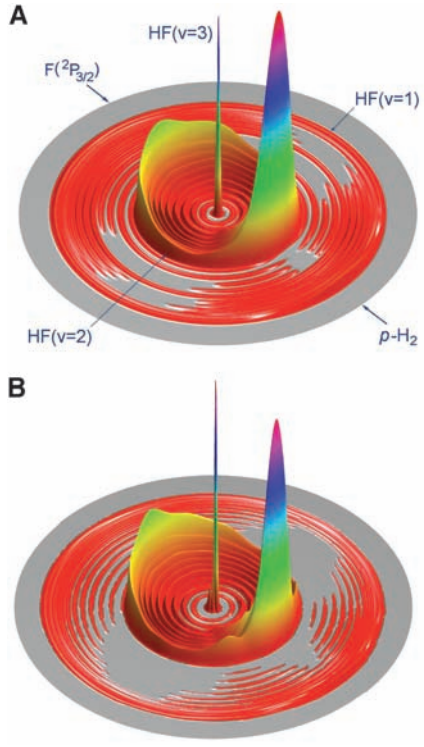

Fig. 2. Experimental (**A**) and theoretical (**B**) 3D contour plots for the product translational energy and angle distributions for the $F(^2P_{3/2}) + H_2(j = 0)$ reaction at the collision energy of 0.52 kcal/mol. The different circles represent different HF product ro-vibrational states. The forward-scattering direction for HF is defined along the F atom beam direction.

the delayed appearance of the HF($v' = 3$), the inclusion of spin-orbit interaction, and the assignment of the resonances (*20*). On the basis of modifications of the SW-PES at the exit channel, a new PES (SWMHS-PES) was recently developed for the $F + H_2$ reaction (*20*). The picture of reaction resonances at low collision energies on the SWMHS-PES is substantially different from that on the SW-PES. Clearly, a consensus physical picture of reaction resonances in this benchmark system has not yet emerged.

In an effort to resolve the controversy, we have carried out a full quantum-state resolved crossed-beam scattering study on the $F + H_2$ reaction, with the use of the high-resolution and highly sensitive H-atom Rydberg tagging method (*21*). State-to-state scattering studies have recently provided great insights into the dynamics of elementary chemical reactions (*22*–*25*). We also modeled the reaction in a full quantum scattering study, based on a highly accurate PES constructed for this purpose, which includes the spin-orbit interaction with small empirical corrections (*26*). Because the F* atom in the first electronic excited state $^2P_{1/2}$ is about 400 cm^{-1} higher in energy than the ground state $F(^2P_{3/2})$, the resolution (about 1% in energy, or roughly 20 cm^{-1} at the translational energy $E_t = 2000$ cm^{-1}) in this work can easily distinguish the $F(^2P_{3/2})$ and $F^*(^2P_{1/2})$ reactions. All the main signals observed and analyzed here were attributed to the ground-state F atom reaction.

Time-of-flight (TOF) spectra of the H atom products from the $F + H_2$ reaction were measured at many laboratory angles at 5° intervals, with the collision energy fixed at 0.52 kcal/mol (Fig. 1). The main structures in these TOF spectra can be clearly assigned to the HF product ro-vibrational states from the ground-state $F(^2P_{3/2})$ reaction with $H_2(j = 0)$. The spectra were then converted to the center-of-mass frame, using a standard Jacobian transformation, to obtain the product kinetic energy distributions. During the conversion, detection efficiencies of the H atom product at different laboratory angles and different velocities were simulated and included. The kinetic energy distributions obtained experimentally in the laboratory frame were fitted by simply adjusting the relative populations of the ro-vibrational states of the HF product. From these fittings, relative population distributions of the HF product at each ro-vibrational state were determined at 36 laboratory angles at the collision energy of 0.52 kcal/mol. Quantum-state distributions of the HF product in the center-of-mass frame ($\Theta_{cm} = 0°$ to 180°) were then determined by a polynomial fit to the above results, and from these distributions, full ro-vibrational state–resolved differential cross section (DCS) values were determined (Fig. 2A).

At this collision energy, all HF($v' = 1, 2, 3$) products were observed. The observation of the HF($v' = 3$) product (the middle sharp peak in Fig. 2A) suggests that the HF($v' = 3$) product appears as soon as the collision energy reaches this channel's threshold. This result is consistent with previous experimental results at higher collision energies and is considerably different from the result predicted by the SW-PES, in which the HF($v' = 3$) product does not appear below collision energies of 1 kcal/mol. Another intriguing observation from this experiment is the pronounced forward-scattering peak (referenced to the F beam) for the HF($v' = 2$) product, which was not observed previously because of the experimental difficulty in accessing the low collision energy region and in measuring the DCS for this reaction. The forward-scattered product is potentially an important probe of reaction resonances, because forward reactive scattering could relate closely to the time delay caused by resonance-state trapping (*4*, *23*).

We also carried out a careful measurement of the DCS collision energy dependence for the HF($v' = 2$) product in the forward-scattering direction. The detector was fixed in the forward direction at different collision energies, and the measurement was repeated 10 times at different collision energies to reduce experimental error, which was estimated to be about 10%. The data in the collision energy range of 0.2 to 0.9 kcal/mol show a peak for the forward-scattering HF($v = 2$) product at the collision energy of 0.52 kcal/mol (Fig. 3A).

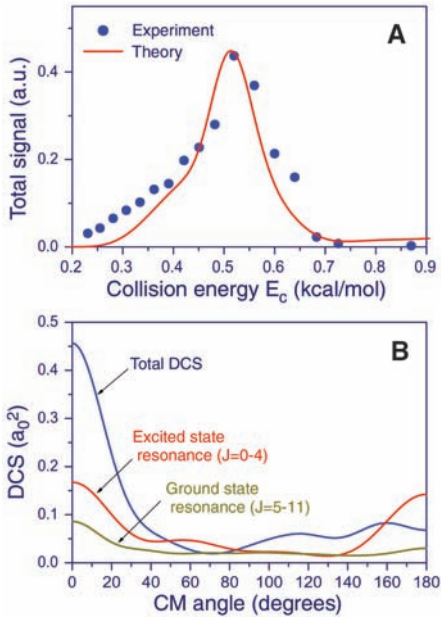

Fig. 3. (**A**) Collision energy–dependent DCS for the forward-scattering HF(v' = 2) product. A resonance-like peak is clearly observed at the collision energy of 0.52 kcal/mol. The solid circles are the experimental data, and the solid line is the calculated theoretical result. (**B**) The total DCS of the HF(v' = 2) product and the DCS contributions to the HF(v' = 2) product from both the ground and the excited resonance partial waves at 0.52 kcal/mol.

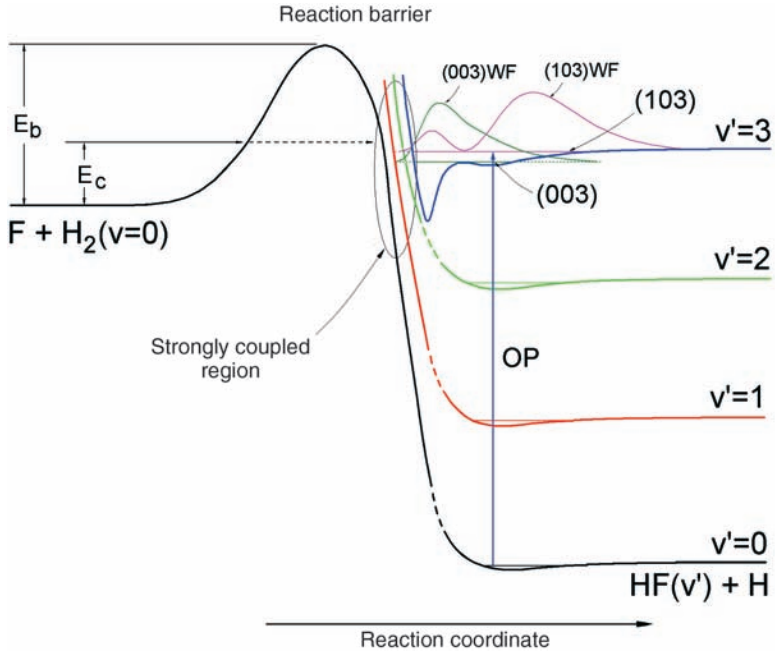

Fig. 4. Schematic diagram showing the resonance-mediated reaction mechanism for the F + H_2 reaction with two resonance states trapped in the peculiar HF(v' = 3)-H′ VAP well. The 1D wave functions of the two resonance states are also shown. The (003) state is the ground resonance state; the (103) resonance is the first excited resonance state. Calculated van der Waals states for the lower VAPs are also shown. OP, overtone pumping; E_b, barrier height; E_c, collision energy.

To interpret these data, we constructed a highly accurate PES for the F($P_{3/2}$) + H_2 reaction. We used the internally contracted multireference configuration interaction method (*27*, *28*) with the Davidson correction (icMRCI + Q) (*29*) and the augmented correlation-consistent valence 5-zeta (aug-cc-pv5z) basis set of Dunning (*30*). [For a detailed description of the PES construction, see (*26*).] The static barrier for the reaction was calculated to be 2.33 kcal/mol. On the basis of this PES, fully converged quantum scattering calculations were carried out for the F($P_{3/2}$) + H_2(j = 0) reaction at collision energies up to 1.5 kcal/mol using the ABC code (*31*). All the theoretical results shown here are convoluted with the experimental collision energy spread. The calculations support predominantly forward-scattered HF(v' = 2) products at a collision energy of 0.52 kcal/mol. The overall agreement between the theoretical and experimental data is very good (Fig. 2), which is remarkable given that the DCS varies rapidly around 0.52 kcal/mol. Thus, the new PES is clearly accurate from the dynamical point of view. We also compared theoretical and experimental DCSs at other collision energies, and the agreement is also generally good. Theoretical results show that the HF(v' = 3) product (the middle sharp peak in Fig. 2B) is already abundant at 0.52 kcal/mol, in good agreement with the current experimental observation. This agreement shows clear progress from simulations based on previous potential energy surfaces.

We also calculated the collision energy dependence for the forward-scattering HF(v' = 2) product (Fig. 3A), and the result mirrors the experimental result. It is obvious that the theoretical result is very similar to the experimental data, with a clear narrow peak precisely at 0.52 kcal/mol. Small empirical corrections, which scaled the ab initio calculated energies so that the asymptotic energetics matched the correct experimental values, rendered the theoretically predicted resonance peak in almost perfect agreement with the current experimental result. With these corrections, the predicted DCS is also in excellent agreement with the experimental DCS at the same collision energies.

The nature of the narrow resonant peak for the forward-scattered HF(v' = 2) product is very intriguing. The energy-dependent reaction probability (*32*) (fig. S1) for the total angular momentum J = 0 exhibits two distinctive peaks, at 0.26 and 0.46 kcal/mol, that correspond to two reaction resonance states: the ground and the excited resonance states. Partial wave analysis shows that about 65% of the reaction cross section at 0.52 kcal/mol comes from the excited resonance with contributions from the J = 0 to 4 partial waves, whereas the other 35% is due to the ground resonance with contributions from J = 5 to 11 (*32*) (figs. S2 and S3). Figure 3B shows the total DCS and the DCS contributions from both the ground and the excited resonance partial waves at 0.52 kcal/mol. Clearly, the excited resonance plays a major role in the HF(v' = 2) forward scattering, but the ground resonance is also important. More interestingly, it seems that the partial waves from both resonances interfere constructively, making the forward-scattering HF(v' = 2) peak much more pronounced than the mere summation of the DCS contributions from the ground and the excited resonances. The narrow peak for the HF(v' = 2) forward scattering at the collision energy of 0.52 kcal/mol (Fig. 3A) is thus directly related to the constructive quantum interference between the two reaction resonance pathways.

From the converged time-dependent wave packet calculations, the exact scattering wave functions at 0.26 and 0.46 kcal/mol for J = 0 are extracted. The three-dimensional (3D) scattering wave function at the collision energy of 0.26 kcal/mol shows the existence of three nodes along the H-F coordinate (correlating to the HF product) in the HF-H′ complex with no node along the reaction coordinate (*32*) (fig. S4). The projection of the J = 0 scattering wave function at 0.26 kcal/mol to the HF vibrational states shows that the main character in this wave function is HF(v' = 3) with the outgoing waves mostly on HF(v' = 2) (*32*) (fig. S5). This implies that the resonance state at 0.26 kcal/mol is the ground resonance state, (003), trapped in the HF(v' = 3)-H′ vibrational adiabatic potential (VAP) well. The 3D scattering wave function for J = 0 at the collision energy of 0.46 kcal/mol shows the existence of three nodes along the H-F coordinate (correlating to the HF product) in the HF-H′ complex with one node along the

reaction coordinate (*32*) (fig. S4). The projection of the $J = 0$ scattering wave function at 0.46 kcal/mol to the HF vibrational states shows the main character in this wave function is predominantly HF($v' = 3$) with the outgoing waves also mostly on HF($v' = 2$) (*32*) (fig. S5). This suggests that the resonance state at 0.46 kcal/mol is the excited reaction resonance state trapped in the HF($v' = 3$)-H′ VAP well. This resonance state can be assigned to the (103) resonance state with one-quantum vibration along the reaction coordinate, zero-quantum vibration on the bending motion (or hindered rotation), and three-quanta vibration along the HF stretching.

Figure 4 shows the resonance-mediated reaction mechanism. The HF($v' = 3$)-H′ VAP on the new PES is very peculiar with a deeper vibrational adiabatic well close to the reaction barrier and a shallow van der Waals (vdW) well, which is similar to the picture on the SW-PES (*33*) and different from that on the SWMHS-PES (*20*). The 1D wave function for the ground resonance state in Fig. 4 shows that this state is mainly trapped in the inner deeper well of the HF($v' = 3$)-H′ VAP with a considerable vdW character, whereas the excited resonance wave function is mainly a vdW resonance. The main character of the ground resonance state is similar to that of the observed resonance in the F-H-D reaction (*15*), but with some difference because of the vdW character in the F-H-H case. Because of the vdW characters, these two resonance states could likely be accessed via overtone pumping from the HF($v' = 0$)-H′ vdW well. The above analysis also suggests that the vdW interaction can affect the reaction dynamics in a substantial way (*17*, *34*).

References and Notes

1. G. C. Schatz, *Science* **288**, 1599 (2000).
2. A. Kuppermann, in *Potential Energy Surfaces and Dynamical Calculations*, D. Truhlar, Ed. (Plenum, New York, 1981), pp. 375–420.
3. Y. T. Lee, *Science* **236**, 793 (1987).
4. K. Liu, *Annu. Rev. Phys. Chem.* **52**, 139 (2001).
5. F. Fernandez-Alonso, R. N. Zare, *Annu. Rev. Phys. Chem.* **53**, 67 (2002).
6. G. C. Schatz, J. M. Bowman, A. Kuppermann, *J. Chem. Phys.* **58**, 4023 (1973).
7. G. C. Schatz, J. M. Bowman, A. Kuppermann, *J. Chem. Phys.* **63**, 674 (1975).
8. G. C. Schatz, J. M. Bowman, A. Kuppermann, *J. Chem. Phys.* **63**, 685 (1975).
9. S.-F. Wu, B. R. Johnson, R. D. Levine, *Mol. Phys.* **25**, 839 (1973).
10. D. M. Neumark, A. M. Wodtke, G. N. Robinson, C. C. Hayden, Y. T. Lee, *Phys. Rev. Lett.* **53**, 226 (1984).
11. D. M. Neumark, A. M. Wodtke, G. N. Robinson, C. C. Hayden, Y. T. Lee, *J. Chem. Phys.* **82**, 3045 (1985).
12. F. J. Aoiz *et al.*, *Chem. Phys.* **223**, 215 (1994).
13. J.-F. Castillo, D. E. Manolopoulos, K. Stark, H.-J. Werner, *J. Chem. Phys.* **104**, 6531 (1996).
14. K. Stark, H.-J. Werner, *J. Chem. Phys.* **104**, 6515 (1996).
15. R. T. Skodje *et al.*, *Phys. Rev. Lett.* **85**, 1206 (2000).
16. D. E. Manolopoulos *et al.*, *Science* **262**, 1852 (1993).
17. C. L. Russell, D. E. Manolopoulos, *Chem. Phys. Lett.* **256**, 465 (1996).
18. L. Y. Rusin, M. B. Sevryuk, J. P. Toennies, *J. Chem. Phys.* **122**, 134314 (2005).
19. S. A. Nizkorodov, W. W. Harper, W. B. Chapman, B. W. Blackmon, D. J. Nesbitt, *J. Chem. Phys.* **111**, 8404 (1999).
20. M. Hayes, M. Gustafsson, A. M. Mebel, R. T. Skodje, *Chem. Phys.* **308**, 259 (2005).
21. L. Schnieder, K. Seekamp-Rahn, E. Wrede, K. H. Welge, *J. Chem. Phys.* **107**, 6175 (1997).
22. X. Liu, J. J. Lin, S. A. Harich, G. C. Schatz, X. Yang, *Science* **289**, 1536 (2000).
23. S. A. Harich *et al.*, *Nature* **419**, 281 (2002).
24. D. Dai *et al.*, *Science* **300**, 1730 (2003).
25. B. R. Strazisar, C. Lin, H. F. Davis, *Science* **290**, 958 (2000).
26. See supporting material on *Science* Online.
27. H.-J. Werner, P. J. Knowles, *J. Chem. Phys.* **89**, 5803 (1988).
28. P. J. Knowles, H.-J. Werner, *Chem. Phys. Lett.* **145**, 514 (1988).
29. S. R. Langhoff, E. R. Davidson, *Int. J. Quantum Chem.* **8**, 61 (1974).
30. T. H. Dunning, *J. Chem. Phys.* **90**, 1007 (1989).
31. D. Skouteris, J. F. Castillo, D. E. Manolopoulos, *Comput. Phys. Commun.* **133**, 128 (2000).
32. See fig. S1 for the $J = 0$ reaction probability, fig. S2 for the J-shifting reaction probability curves, fig. S3 for the partial wave decomposition of the HF($v' = 2$) forward-scattering peak at the collision energy of 0.52 kcal/mol, fig. S4 for the 3D scattering wave functions at 0.26 and 0.46 kcal/mol for $J = 0$ from converged time-dependent wave packet calculations, and fig. S5 for projection of $J = 0$ scattering wave function at the collision energy of 0.26 kcal/mol (corresponding to the ground resonance state) to HF vibrational states and at 0.46 kcal/mol (corresponding to the excited resonance state).
33. S. D. Chao, R. T. Skodje, *J. Chem. Phys.* **113**, 3487 (2000).
34. T. Xie, D. Wang, J. M. Bowman, D. E. Manolopoulos, *J. Chem. Phys.* **116**, 7461 (2002).

35. Supported mainly by the Chinese Academy of Sciences, the Ministry of Science and Technology, and the National Natural Science Foundation of China. M.G. and R.T.S. acknowledge the support of Academia Sinica. We thank K. Liu for many insightful discussions, and C. Zhou, W. Dong, and X. Wang for their help during the experiment.

Supporting Online Material

www.sciencemag.org/cgi/content/full/311/5766/1440/DC1
Materials and Methods
Figs. S1 to S5
References

5 December 2005; accepted 3 January 2006
10.1126/science.1123452

Signatures of H_2CO Photodissociation from Two Electronic States

H. M. Yin,[1] S. H. Kable,[1]* X. Zhang,[2] J. M. Bowman[2]*

Even in small molecules, the influence of electronic state on rotational and vibrational product energies is not well understood. Here, we use experiments and theory to address this issue in photodissociation of formaldehyde, H_2CO, to the radical products H + HCO. These products result from dissociation from the singlet ground electronic state or the first excited triplet state (T_1) of H_2CO. Fluorescence spectra reveal a sudden decrease in the HCO rotational energy with increasing photolysis energy accompanied by substantial HCO vibrational excitation. Calculations of the rotational distribution using an ab initio potential energy surface for the T_1 state are in very good agreement with experiment and strongly support dominance of the T_1 state in the dynamics at the higher photolysis energies.

The study of reaction dynamics of small molecules has contributed greatly to our understanding of molecular reactivity—an understanding that now allows us to follow and even control reactions from precise quantum states of a reactant to the quantum states of the products. However, even for molecules as small as four atoms, the influence of different electronic states on the product state distributions is not well understood. Here we examine this issue for the otherwise very well studied photodissociation of the tetra-atomic formaldehyde molecule (H_2CO).

Formaldehyde is found in the troposphere as a result of air pollution. It decomposes via photodissociation due to absorption of actinic solar radiation (*1*). Although this process might seem to represent a simple chemical reaction, there are at least six different photochemical and photophysical pathways that could occur after absorption of a near-ultraviolet photon excites H_2CO to its lowest excited singlet electronic state (Fig. 1). These processes include fluorescent relaxation; internal conversion to a vibrationally excited electronic ground state (S_0), which in turn results in dissociation to radical or molecular products; or intersystem crossing to a triplet electronic state, also followed by dissociation to radical products.

The fluorescence and S_0 dissociative pathways to the radical and molecular products have a long history, with much of the pioneering work done by Moore and Weisshaar (*2*). Knowledge of the respective branching ratios (or quantum yields) is vital to atmospheric modeling. An alternative route to molecular products from S_0, via a "roaming atom" mechanism (*3*), was reported in 2004 (*4*). An isomerization pathway on S_0 has been predicted (*5*, *6*) but not observed experimentally.

Reaction via the triplet channel has also long been suspected, although its precise threshold energy and probability are not well established.

[1]School of Chemistry, University of Sydney, Sydney, NSW 2006, Australia. [2]Department of Chemistry and Cherry L. Emerson Center for Scientific Computation, Emory University, Atlanta, GA 30322, USA.

*To whom correspondence should be addressed. E-mail: s.kable@chem.usyd.edu.au (S.H.K.), jmbowma@emory.edu (J.M.B.)

Observation of Feshbach Resonances in the F + H_2 → HF + H Reaction

Minghui Qiu, Zefeng Ren, Li Che, Dongxu Dai, Steve A. Harich, Xiuyan Wang, Xueming Yang, Chuanxiu Xu, Daiqian Xie, Magnus Gustafsson, Rex T. Skodje, Zhigang Sun and Dong H. Zhang

Science **311** (5766), 1440-1443.
DOI: 10.1126/science.1123452